

Application of the Kalman Filters in the Self-Commissioning High-Performance Drive System with an Elastic Joint

Krzysztof Szabat and Teresa Orłowska-Kowalska
*Wrocław University of Technology
Poland*

1. Introduction

Torsional vibrations limit the performance of many industrial drives. They decrease the system reliability, product quality in some specific cases they can even lead to instability of the whole control structure. The problem of damping of torsional vibrations originates from the rolling-mill drive, where large inertias of the motor and load parts with a long shaft create an elastic system (Hori et al., 1999), (Szabat & Orłowska-Kowalska 2007), (Pittner & Simaan, 2008). Similar problems exist in paper and textile industry, where the electromagnetic torque goes through complex mechanical parts of the drive (Valenzuela et al., 2005). The damping ability of the system is also a critical issue in conveyer and cage-host drives (Hace et al., 2006). Originally the elastic system has been recognized in high-power applications. However, due to the progress in power electronic and microprocessor systems, which allow controlling the electromagnetic torque almost without delay, the torsional vibrations appear in many medium and small power applications. Today they are acknowledged in servo-drives, throttle drives, robot arm drives including space applications, and others (Hamamoto et al., 2003), (O'Sullivan et al., 2007), (Shen & Tsai, 2006), (Katsura & Ohnishi, 2005) and (Vasak et al., 2007).

Since the classical PI controller is not effective in the two-mass drive system different control concepts have been developed. As has been shown in (Zhang & Furusho, 2000), the application of the PID controller ensures effective suppression of the torsional vibrations. This approach is easy to implement and designated for the system with an accurate speed sensor. Torsional vibrations can be damped effectively by inserting additional feedback from selected state variable(s) of the two-mass system. The survey of those structures is presented in (Szabat & Orłowska-Kowalska 2007) and (Nordin & Gutman, 2002). The structure with one additional feedback can damp the torsional vibration effectively, yet the settling time of the system cannot be set freely. The more advanced control concept relies on the inserting of all states of the control structure, which allows the free location of the system closed-loop poles. The cascade control structure with two additional feedbacks or the structure with the state controller are illustrated in (O'Sullivan et al., 2007) and (Szabat & Orłowska-Kowalska, 2008).

Also the nonlinear and adaptive control have been proposed to control the two-mass system in order to eliminate the effect of the parameter uncertainties and disturbances e.g. in papers

Source: Kalman Filter: Recent Advances and Applications, Book edited by: Victor M. Moreno and Alberto Pigazo, ISBN 978-953-307-000-1, pp. 584, April 2009, I-Tech, Vienna, Austria

(Erbatur et al., 1999) and (Erenturk, 2008) the sliding mode control have been applied. In all cases the authors claim that the robustness to the parameter variation is one of the major advantages of this type of control. Different way to eliminate the effect of the disturbances is to apply the adaptive control. The application of the Kalman filter in the two-mass drive structure is presented in (Szabat & Orłowska-Kowalska, 2008) and (Hirovonen et al., 2006). The damping of the torsional vibration using adaptive neuro-fuzzy controller has been presented in (Wang & Frayman, 2002), (Szabat & Orłowska-Kowalska, 2008b). In all cases the authors report an improved performance of the controlled drives.

Despite the advantages of the nonlinear and adaptive control, about 95% of all controllers used in the industry rely on the PI concept (Åström & Hägglund, 2001). It results from the following reasons. To begin with, the classical PI concept is well-known by industrial engineers. The tuning methodologies and stability analysis methods are well established. Therefore, the PI-control structure with two additional feedbacks from the shaft torque and difference between the motor and the load speed is selected in this paper to work in the real system (Szabat & Orłowska-Kowalska, 2008). It should be noted that this structure ensures the free location of the system closed-loop poles, which means that the responses of the system can be shaped in the linear range of the system work.

During the design process of the above-mentioned structure the acknowledgment of the value of the system parameters is necessary. However, in industrial application only the mechanical parameters of the motor calculated according to the nominal data are known. The parameters of the shaft and load machine are uncertain or even unknown in many cases. Therefore, the special identification methods have been developed in order to identify the plant parameters (Schutte et al., 1997), (Wertz et al., 1999), (Eker & Vular, 2003), (Schröder et al., 2001) and (Angerer et al., 2004). They can be divided into two different groups. The basic assumption of all methods dedicated to industry is that only the signals of the electromagnetic torque and motor speed are accessible for identification procedure.

The first group encompasses the off-line identification methods. In this methodology the plant is stimulated by specific types of signals and the response of object is saved. Then on the basis of those signals the plant parameters are calculated. This first framework is presented in (Schutte et al., 1997) and (Wertz et al., 1999). In the paper (Schutte et al., 1997), the plant has been stimulated by step signal of the electromagnetic torque. Then from the response (driving motor speed) the oscillation part of the speed has been extracted. Later this part has been transformed into a frequency domain and the resonant frequency of the system has been identified. From the physical relationship of the plant the stiffness coefficient of the plant and the inertia of the load machine have been calculated. In the following work (Wertz et al., 1999) the excitation signal has been changed to the PRBS so as to extracting the additional information from frequency domain, namely the anti-resonant frequency of the plant. On the basis on the values of the antiresonant and resonant frequency all the main parameters of the plant can be calculated (inertia of the motor and load machines, stiffness coefficient). Additionally, by adjusting the frequency characteristics of the model to the plant the internal damping coefficient of the shaft can be determined. The next framework is based on the parametric identification method (Wertz et al., 1999) and (Eker & Vular, 2003). On the basis of the responses of the object, the parameters of the linear model of the plant are selected in order to minimise the difference between the real system and the model outputs. As the advantage of this method, the authors report (Wertz et al., 1999) the possibility of the identification of the friction in the system. However, they

claim the problems with the determination of the order of the model which is the main disadvantage of this method. The application of this method to identification of the multi-mass system is presented in (Eker & Vular, 2003). The authors report good accuracy of the estimated parameters.

The second group includes so-called the on-line identification methods, in which special observers are applied to calculate the plants parameters in the real time. In (Szabat & Orłowska-Kowalska, 2008) the mechanical parameters are estimated on-line with the help of the Kalman filter. The obtained results show the advantages of the proposed estimation technique. A different approach is presented in (Schröder et al., 2001). The so-called intelligent observers have been used to identify the nonlinear parts of the system. Nevertheless, the parameters of the linear parts have to be known exactly. The extension of the mentioned works has been presented in (Angerer et al., 2004). The assumed parameter of the linear parts can be incorrect (up to 20% of errors is acceptable). Additionally the existence of the some delay elements in the nonlinear part is acceptable.

The main goal of the paper is to present the application of the Kalman filters in the self-commissioning high-performance drive system with an elastic joint. Two main topic are discussed in the paper. Firstly the issues related to estimation of the mechanical parameters of the drives are discussed. The nonlinear extended Kalman filter is applied for this purpose. Then on the basis of the obtained parameters the advanced control structures with two additional feedbacks is designed. In order to provide the information of the non-measurable state variables (shaft torque, load speed) the linear Kalman filter is applied. The drive system is tested under different conditions. The theoretical considerations and simulation works are supported by the experimental results.

2. The mathematical model of the two-mass system and the control structure

In the paper the commonly-used model of the drive system with the resilient coupling is considered. The system is described by the following state equation (in per unit system) (Szabat & Orłowska-Kowalska, 2007):

$$\frac{d}{dt} \begin{bmatrix} \omega_1(t) \\ \omega_2(t) \\ m_s(t) \end{bmatrix} = \begin{bmatrix} 0 & 0 & -\frac{1}{T_1} \\ 0 & 0 & \frac{1}{T_2} \\ \frac{1}{T_c} & -\frac{1}{T_c} & 0 \end{bmatrix} \begin{bmatrix} \omega_1(t) \\ \omega_2(t) \\ m_s(t) \end{bmatrix} + \begin{bmatrix} \frac{1}{T_1} \\ 0 \\ 0 \end{bmatrix} [m_e] + \begin{bmatrix} 0 \\ -\frac{1}{T_2} \\ 0 \end{bmatrix} [m_L] \quad (1)$$

where: ω_1 - motor speed, ω_2 - load speed, m_e - motor torque, m_s - shaft (torsional) torque, m_L - disturbance torque, T_1 - mechanical time constant of the motor, T_2 - mechanical time constant of the load machine, T_c - stiffness time constant. The nominal values are $T_1=T_2=203\text{ms}$ and $T_c=2.6\text{ms}$.

A typical electrical drive system is composed of a power converter-fed motor coupled to a mechanical system, a microprocessor-based controllers, current, rotor speed and/or position sensors used as feedback signals. Typically, a cascade speed control structure containing two major control loops is used, as presented in Fig 1.

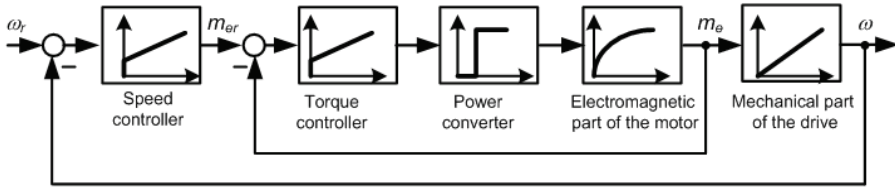


Fig. 1. The classical cascade control structure

The inner control loop performs the motor torque regulation and consists of the power converter, electromagnetic part of the motor, current sensor and respective current or torque controller. As this control loop is designed to provide sufficiently fast torque control, it can be approximated by an equivalent first order term. If the suitable torque control is ensured, the driven machine could be an AC or DC motor, with no difference in the outer speed control loop. The outer loop consists of the mechanical part of the motor, speed sensor, speed controller, and is cascaded to the inner loop. It provides speed control according to the reference value. The classical structure (without additional feedbacks) works well only for specific inertia ratio (T_2/T_1) of the two-mass system. When the mechanical time constant of the load machine is low, transients of the system are not proper. To improve the dynamical characteristics of the drive, a modification of the cascade structure is necessary. It is obtained by inserting to the control structure the additional feedbacks from selected state variables (Szabat & Orłowska-Kowalska, 2007) and (Szabat & Orłowska-Kowalska, 2008). The pattern of the speed control structure for the two-mass system with a simplified inner control loop and additional feedbacks from the shaft torque and the difference between the motor and load speed is presented in Fig 2.

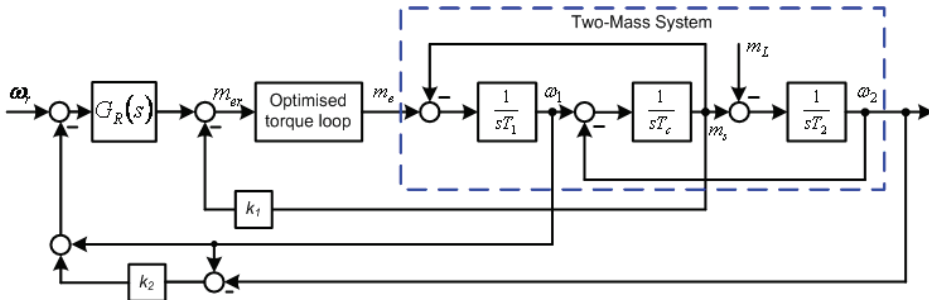


Fig. 2. Schematic diagram of the control structure with additional feedbacks

The closed-loop transfer functions from reference input to the motor and load speed are given by the following equations (with the assumption that the optimized transfer function of the electromagnetic torque control loop equals 1):

$$G_{\omega_1}(s) = \frac{\Delta\omega_1(s)}{\Delta\omega_r(s)} = \frac{G_r(s^2T_2T_c + 1)}{s^3T_1T_2T_c + s^2T_2T_cG_r(1+k_2) + s(T_1+T_2(1+k_1)) + G_r} \tag{2}$$

$$G_{\omega_2}(s) = \frac{\Delta\omega_2(s)}{\Delta\omega_r(s)} = \frac{G_r}{s^3T_1T_2T_c + s^2T_2T_cG_r(1+k_2) + s(T_1+T_2(1+k_1)) + G_r} \tag{3}$$

where:

$$G_r = K_p + K_I / s \tag{4}$$

is the transfer function of the controller.

The parameters of the control structures are set using the pole-placement method, according to the following equations (Szabat & Orłowska-Kowalska, 2008):

$$K_I = \omega_0^4 T_1 T_2 T_c \tag{5}$$

$$K_p = 4 \xi_r \omega_0^3 T_1 T_2 T_c \tag{6}$$

$$k_2 = (\omega_0^2 T_2 T_c)^{-1} - 1 \tag{7}$$

$$k_1 = T_1 T_2^{-1} (4 \xi_r^2 - k_2) (1 + k_2)^{-1} - 1 \tag{8}$$

where: ξ_r - required damping coefficient, ω_0 - required resonant frequency of the system. The cascade control structure with additional feedbacks requires information of the values of the two-mass system parameters and signals from the hard measurable state variables, i.e. shaft torque and load speed. Therefore, the application of state estimators like the state observers or Kalman Filters is advisable.

3. Mathematical model of the Kalman filters

3.1 Linear Kalman Filter (LKF)

In the case of the drive system with elastic joint, the state vector of the drive system (1) is extended by the load torque, to obtain the estimation of all mechanical state variables of the system:

$$\mathbf{x}_R = [\omega_1 \quad \omega_2 \quad m_s \quad m_L]^T \tag{9}$$

The motor electromagnetic torque and speed are used as input and output variables of the LKF, respectively:

$$\mathbf{u} = m_e \quad \mathbf{y}_R = \omega_1 \tag{10}$$

The mechanical part of the drive system (1) can be described in the following form, where according to the KF theory, the system is disturbed by Gaussian white noises, which represent process and measurement errors ($\mathbf{w}(t)$, $\mathbf{v}(t)$):

$$\frac{d}{dt} \mathbf{x}_R(t) = \mathbf{A}_R \mathbf{x}_R(t) + \mathbf{B}_R \mathbf{u}(t) + \mathbf{w}(t) = \mathbf{f}_R(\mathbf{x}_R(t), \mathbf{u}(t)) + \mathbf{w}(t) \tag{11a}$$

$$\mathbf{y}_R(t) = \mathbf{C}_R \mathbf{x}_R(t) + \mathbf{v}(t) \tag{11b}$$

Thus the state, control and output matrices of this extended LKF are following:

$$\mathbf{A}_R = \begin{bmatrix} 0 & 0 & -\frac{1}{T_1} & 0 \\ 0 & 0 & \frac{1}{T_2} & -\frac{1}{T_2} \\ \frac{1}{T_c} & -\frac{1}{T_c} & 0 & 0 \\ 0 & 0 & 0 & 0 \end{bmatrix} \quad \mathbf{B}_R = \begin{bmatrix} \frac{1}{T_1} \\ 0 \\ 0 \\ 0 \end{bmatrix} \quad \mathbf{C}_R = \begin{bmatrix} 1 \\ 0 \\ 0 \\ 0 \end{bmatrix}^T \tag{12}$$

After discretisation of Eq. (11) with the sampling step T_p , the state estimation using LKF algorithm is calculated by Eq. (13):

$$\hat{\mathbf{x}}_R(k+1/k+1) = \hat{\mathbf{x}}_R(k+1/k) + \mathbf{K}(k+1)[\mathbf{y}_R(k+1) - \mathbf{C}_R(k+1)\hat{\mathbf{x}}_R(k+1/k)] \tag{13}$$

where the gain matrix \mathbf{K} is obtained by the following numerical procedure:

$$\mathbf{P}(k+1/k) = \mathbf{A}_R(k)\mathbf{P}(k)\mathbf{A}_R^T(k) + \mathbf{Q}(k) \tag{14}$$

$$\mathbf{K}(k+1) = \mathbf{P}(k+1/k)\mathbf{C}_R^T(k+1)[\mathbf{C}_R(k+1)\mathbf{P}(k+1/k)\mathbf{C}_R^T(k+1) + \mathbf{R}(k)]^{-1} \tag{15}$$

$$\mathbf{P}(k+1/k+1) = [\mathbf{I} - \mathbf{K}(k+1)\mathbf{C}_R(k+1)]\mathbf{P}(k+1/k) \tag{16}$$

with state and measurement covariance matrices \mathbf{Q} and \mathbf{R} . The estimation accuracy of the Kalman Filter strictly depends on proper setting of the covariance matrix \mathbf{Q} and \mathbf{R} elements. Usually to solve this problem the trial and error tuning procedure is applied. However, this approach can not guarantee the best selection of the covariance matrices. In this work the covariance matrices \mathbf{Q} and \mathbf{R} were determined using the genetic algorithm (GA) with the following cost function:

$$F = \min \left\{ \sum_1^n (|m_s - m_{se}|) \sum_1^n (|\omega_2 - \omega_{2e}|) \sum_1^n (|m_L - m_{Le}|) \right\} \tag{17}$$

where m_{se} , ω_{2e} , m_{Le} - denote the estimated state variables

3.2 Non-linear Kalman Filter (NKF)

In the presence of the unknown parameters (T_2 and T_c), there is a need to extend the two-mass system state vector (1) with the additional elements $1/T_2$ and $1/T_c$:

$$\mathbf{x}_R(t) = \left[\omega_1(t) \quad \omega_2(t) \quad m_s(t) \quad \frac{1}{T_2}(t) \quad \frac{1}{T_c}(t) \right]^T \tag{18}$$

where T_2 and T_c denotes the time constant of the load side inertia and the stiffness, respectively. The extended, nonlinear state and output equations can be written in the following form:

$$A_R \left(\frac{1}{T_2}(t), \frac{1}{T_c}(t) \right) = \begin{bmatrix} 0 & 0 & \frac{-1}{T_1} & 0 & 0 \\ 0 & 0 & \frac{1}{T_2}(t) & 0 & 0 \\ \frac{1}{T_c}(t) & \frac{-1}{T_c}(t) & 0 & 0 & 0 \\ 0 & 0 & 0 & 0 & 0 \\ 0 & 0 & 0 & 0 & 0 \end{bmatrix} \quad B_R = \begin{bmatrix} \frac{1}{T_1} \\ 0 \\ 0 \\ 0 \\ 0 \end{bmatrix} \quad C_R = \begin{bmatrix} 1 \\ 0 \\ 0 \\ 0 \\ 0 \end{bmatrix}^T \quad (19)$$

The matrix A_R depends on the changeable parameters T_2 and T_c . It means that in every calculation step this matrix must be updated due to the estimated value of those parameters, which means that the linearized state equation (3) must be updated in each calculation step. The input and the output vectors of the Kalman filter are electromagnetic torque and motor speed, respectively. After the discretization of (11) the state estimate is calculated using (13). The gain matrix K is obtained by the following numerical procedure. First, the state vector predictor is calculated:

$$P(k+1/k) = F_R(k)P(k)F_R^T(k) + Q(k) \quad (20)$$

where:

$$F_R(k) = \left. \frac{\partial f_R(\mathbf{x}_R(k/k), \mathbf{u}(k), k)}{\partial \mathbf{x}_p(k/k)} \right|_{\mathbf{x}_R = \hat{\mathbf{x}}_R(k/k)} \quad (20)$$

F_R is the state matrix of the system (3) after its linearization in the actual operating point. It must be updated in every calculation step:

$$F_R = \begin{bmatrix} 1 & 0 & \frac{-T_p}{T_1} & 0 & 0 \\ 0 & 1 & \frac{T_p}{T_2(k)} & T_p m_s(k) & 0 \\ \frac{T_p}{T_c(k)} & \frac{-T_p}{T_c(k)} & 1 & 0 & T_p [\omega_1(k) - \omega_2(k)] \\ 0 & 0 & 0 & 1 & 0 \\ 0 & 0 & 0 & 0 & 1 \end{bmatrix} \quad (22)$$

The NKF gain matrix and the covariance matrix of the state estimation error are calculated using (15) and (16).

In this paper covariance matrix elements are set by means of the genetic algorithm with the following cost function:

$$F = \min \left\{ \left(\sum_1^n |T_s - T_{se}| \right) * \left(\sum_1^n |T_c - T_{ce}| \right) \right\} \quad (23)$$

where T_{se} and T_{2e} denote the estimated value of the system parameters. The cost function defined in this way ensures the optimal setting of covariance matrices \mathbf{Q} and \mathbf{R} for unknown drive parameters.

4. Simulation results

4.1 Identification case (NKF)

In the following section the properties of the proposed identification procedure is investigated. The drive system is working under reverse condition. The electromagnetic torque and the motor speed, used as the input and output vectors of NEKF, are disturbed with white noises. The parameters of the covariance matrices are set with the GA in order to ensure the shortest identification time. The resulting value of the covariance matrices are as follows $\mathbf{R}=10$, $\text{diag}(\mathbf{Q})=[12 \ 2 \ 5 \ 300 \ 10e5]$ The transients of the electromagnetic torque and motor speed during the system operation drive are presented in Fig.3.

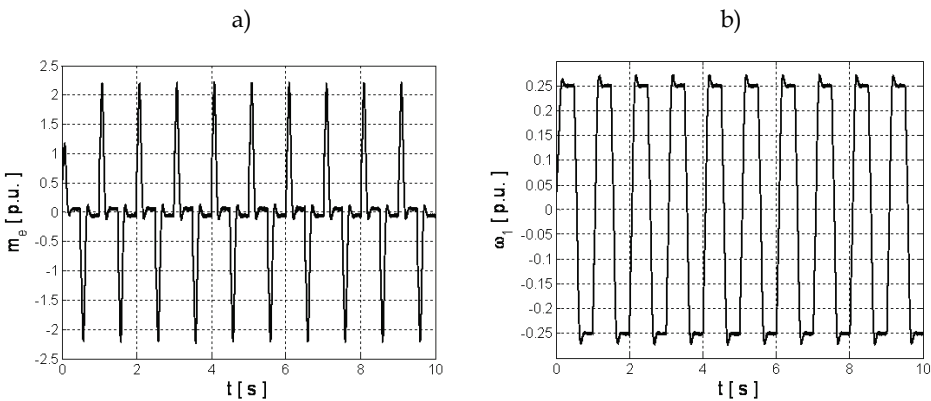


Fig. 3. Transients of the input signal of the Kalman Filter: the electromagnetic torque (a) and the motor speed (b)

The drive system starts with misidentified time constant of the load machine $T_2=406\text{ms}$ and the stiffness time constant $T_c=5.2\text{ms}$ (Fig. 4a,b). During the start-up the estimated value of the T_2 reaches its real value. The value of T_c equals 3.2ms after the first reversal and reaches its real value after 3s. Some small disturbances are visible during every reversal in transients of both estimated parameters.

Then the smaller initial values of the system parameters are tested ($T_2=101.5\text{ms}$, $T_c=1.3\text{ms}$). The input signals of the Kalman filter are presented in Fig. 4. The transients of the estimated parameters are presented in Fig. 4c,d. The values of the covariance matrices \mathbf{Q} and \mathbf{R} are the same as in the previous case (i.e. they are not optimal). During the start-up the time constant of the load machine reaches the value of about 140ms, then after the first reversal it is about 215ms and then slowly converges to its real value. After 3s the estimate of T_2 approaches its real value. The estimated value of the T_c reaches its real value also after 3 s. However, it should be emphasized that the convergence is slower in this case; it can be accelerated by increasing the values of the covariance matrix \mathbf{Q} parameters, which will be demonstrated under experimental study.

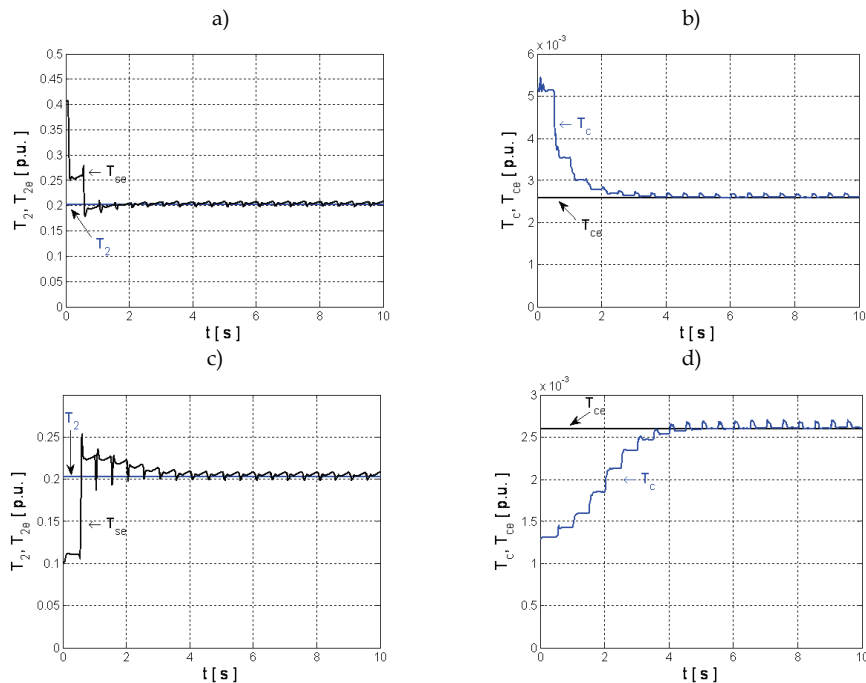


Fig. 4. Transients of the estimated time constant: of the load machine (a,c) and the shaft (b,d) in the case of the bigger (a,b) and smaller (c,d) initial values of those parameters

3.2 Open and closed-loop control structure (LKF)

In the following section the issues related to the application of the LKF are presented. First, the quality of the estimated states is investigated. The electromagnetic torque and the motor speed are taken from the closed-loop control structure. Then in order to emulate the real conditions these signals are disturbed with noises which imitates the measurement sensor quality (5% for the electromagnetic torque and 0.5% for the motor speed). Additionally the values of the parameters used in the Kalman filter are decreased by 3% in order to account for the identification errors. The transients of the input signal of the LKF are presented in Fig. 5.

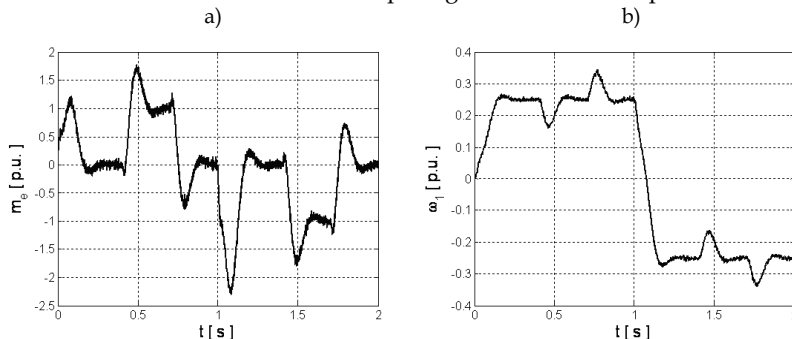


Fig. 5. Transients of the input signal of the Kalman Filter: the electromagnetic torque (a) and the motor speed (b)

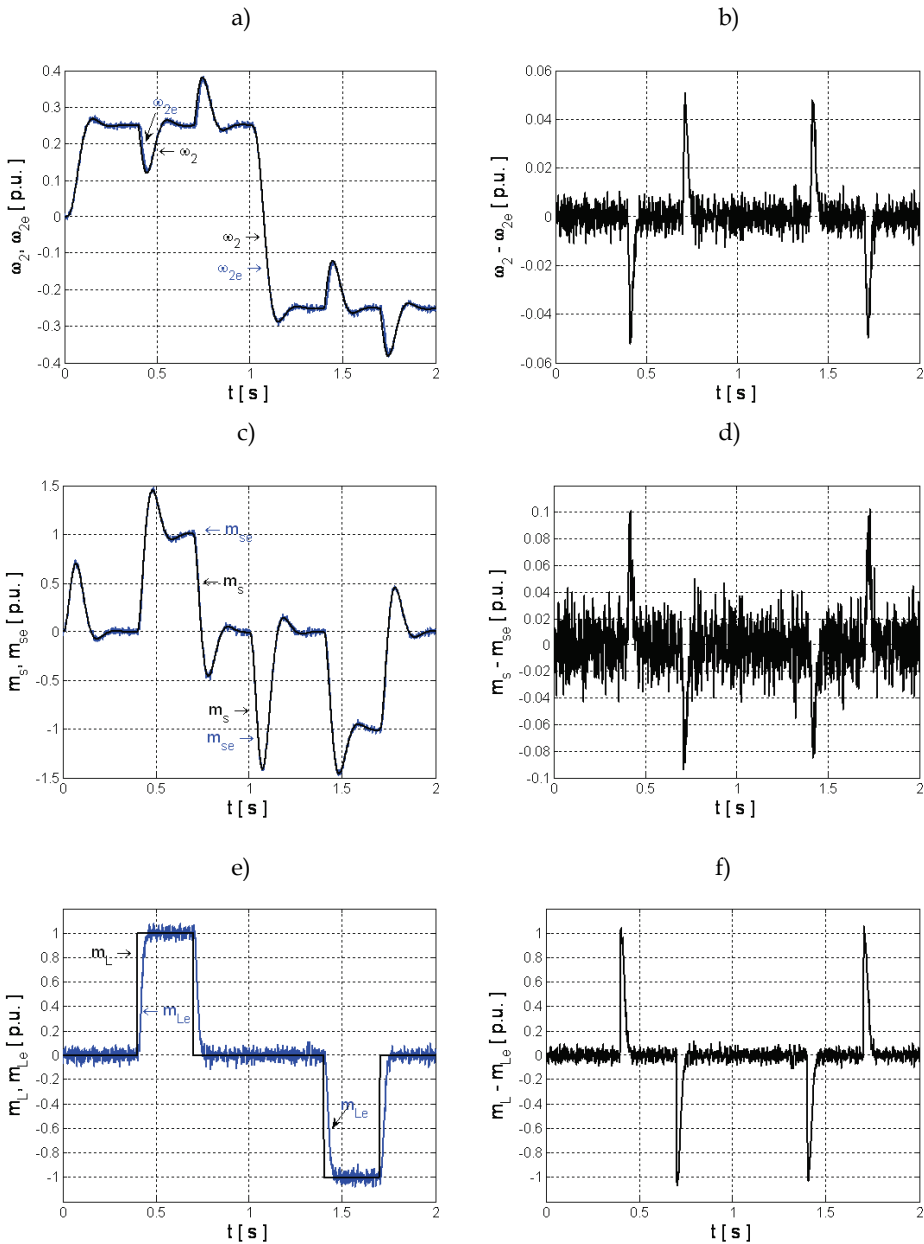


Fig. 6. Transients of the real and estimated variables and their estimation errors: load speed (a,b), shaft torque (c,d) and load torque (e,f) for the closed-loop system with measured and estimated variables

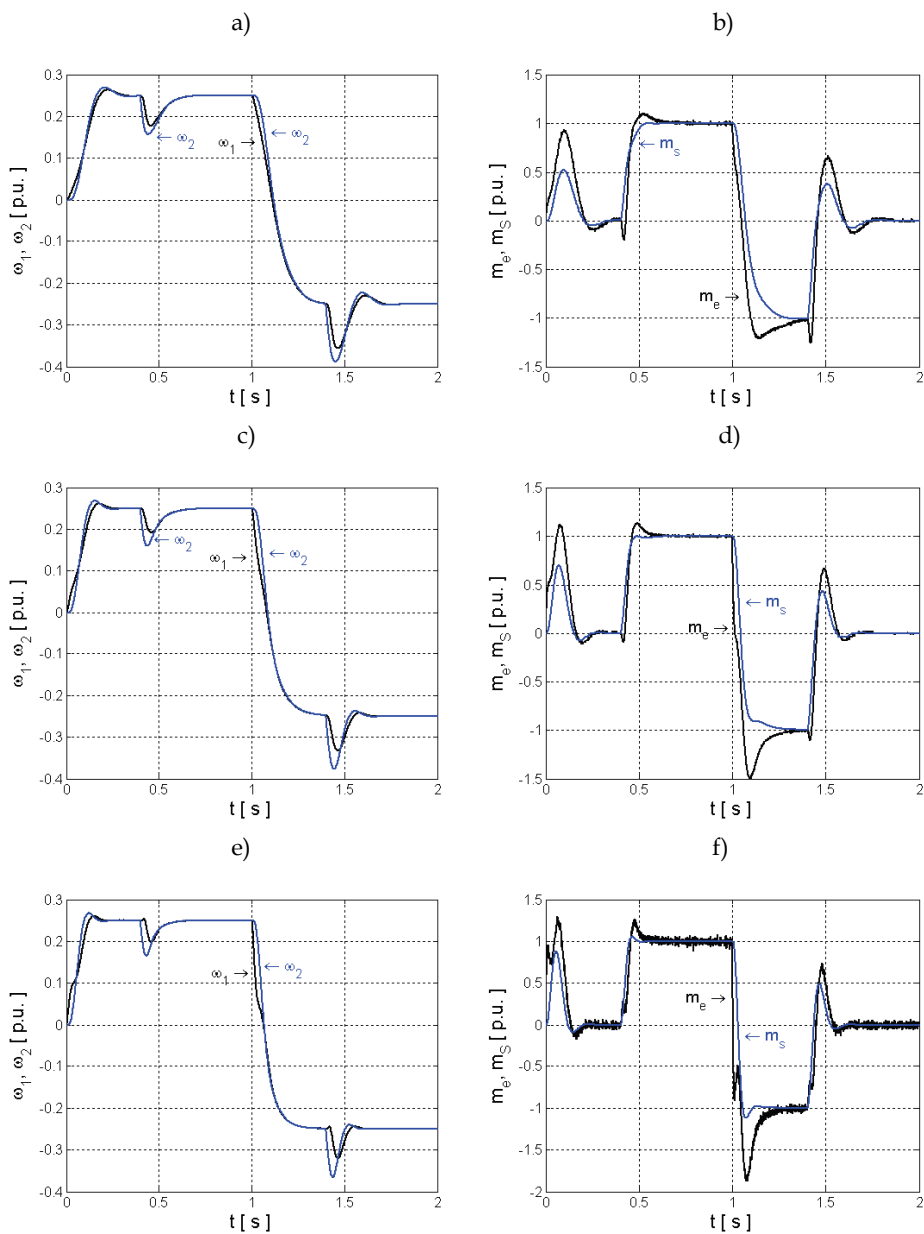


Fig. 7. Transients of the motor and the load speeds (a,c,e) and the electromagnetic and the shaft torques (b,d,f) in the control structure working with the Kalman filter for $\zeta_r=0.7$ and $\omega_0=30\text{s}^{-1}$ (a,b), $\omega_0=40\text{s}^{-1}$ (c,d) i $\omega_0=50\text{s}^{-1}$ (e,f)

The LKF is working in the open-loop structures. The real and estimated system states as well as the estimation errors are presented in Fig. 6.

The LKF works properly. The reconstructed values of the states cover the real ones with small errors. The biggest estimation errors exist in all system state variables in the case of the rapid changing of the load torque. The faster covariance between the real and estimated parameters can be obtained by increasing the values of the covariance matrices. However, at the same time the noise level during the steady-stay condition will increase.

Next the closed-loop control structure (Fig. 8) working with the Kalman filter has been tested. The additional signals from the shaft torque and the load speed are taken from the estimator. The transients of the system for assumed values of the control structure parameters $\zeta_r=0.7$ and $\omega_0=30s^{-1}(a,b)$, $\omega_0=40s^{-1}(a,b)$, $\omega_0=50s^{-1}(a,b)$ are presented in Fig. 7.

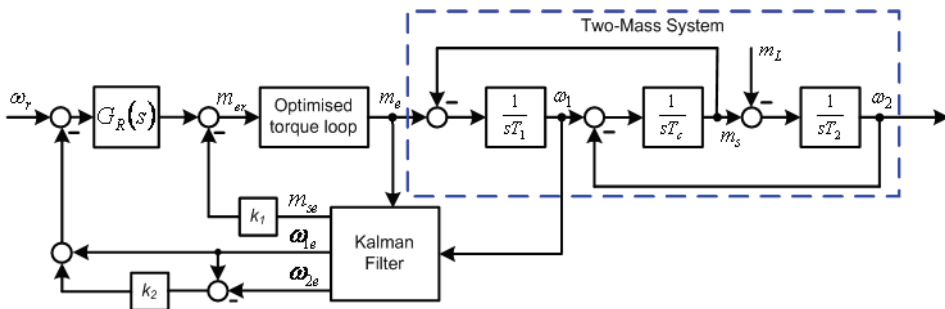


Fig. 8. Schematic diagram of the control structure with LKF

The drive system working under the reverse condition with the reference speed set to the $\omega_r=0.25$ is tested. After the start-up, at the time $t_1=0.4s$ the nominal load torque is applied to the system. Next at the time $t_2=1s$ the reference signal is changing to $\omega_r=-0.25$. Under the reversal the passive load torque is applied to the system. Later at the time $t_3=1.4s$ the load torque is switched off. The drive system works properly. The bigger assumed value of the resonant frequency, the shorter setting time obtained. In the transients of the electromagnetic torque some noises are visible. Their amplitude increases for the bigger values of the resonant frequency. It comes from the fact that the bigger value of the resonant frequency requires the bigger value of the coefficients (k_1, k_2), which gain the noises from the estimated variables.

5. Experimental results

5.1 Experimental set-up

In this section the experimental validation of the analysed algorithms are presented. The laboratory set-up is composed of the two DC-motors (500W each) connected by long shaft. The driving motor is supplied by the power converter. The speeds of the two motors are measured by two incremental encoders (36000 per rotation). The signal from the second encoder is not used in the control structure but only to display the real velocity of the load machine. The current of the motor is measured by LED sensor. The identification and the control algorithms are implemented by digital signal processor using DSpace 1102 control card. The schematic diagram of the control structure is presented in Fig 9.

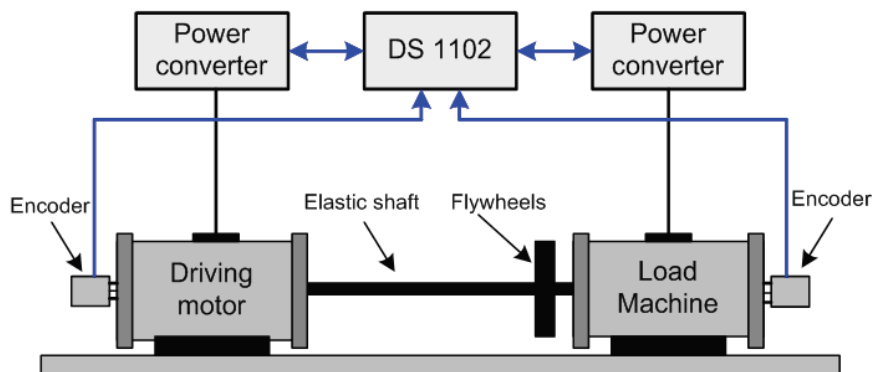


Fig. 9. The schematic diagram of laboratory set-up

5.2 Identification case (NKF)

First the identification procedure has been tested. Similarly as in the simulation study the drive system is stimulated by the square-type of the reference speed signal. The signals of the electromagnetic torque and the motor speed (Fig. 10a,b) are passed to the Kalman Filter. On the basis on these signals the estimated procedure is carried out. The value of the parameters standing for the real one (in the Fig. 10) have been obtained using different identification methodology as presented in (Wertz et al., 1999).

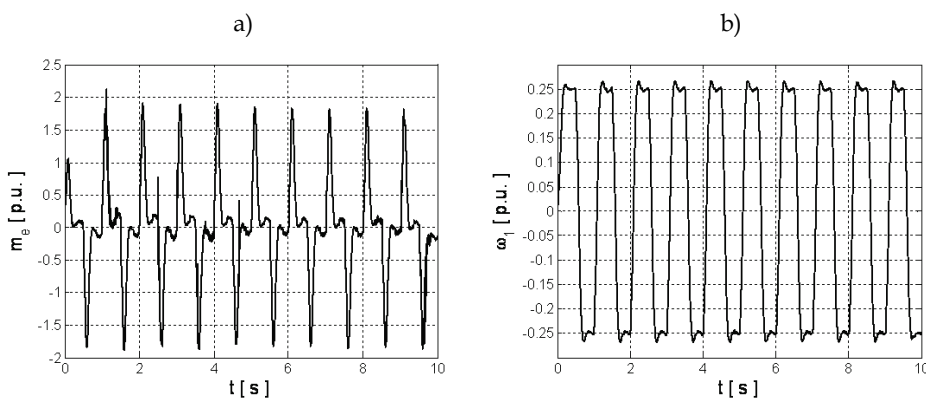


Fig. 10. Transients of the input signal of the Kalman Filter: the electromagnetic torque (a) and the motor speed (b)

Transients of the identified parameters T_2 and T_c are presented in Fig 11. The transients marked as $q_{55}=10e5$ represent the case of the optimal (found by GA) values of the covariance matrices. First the case of the bigger initial values of the identified parameters is considered (Fig. 11a,b). As in the simulation study the estimate of the T_2 tends to its real value very fast. The convergence of T_c is slower. It can be accelerated by increasing the value of the covariance matrix Q . This case is marked in Fig. 11 as $q_{55}=10e6$. However, the increasing the value of q_{55} can bring about the stability problem of the KF algorithm as well as it gain the

disturbances visible in the transients in every reversal. Then the case of the smaller initial value of the mechanical parameters is considered (Fig. 11c,d). Similarly as in the simulation study the identification process is slower. Especially the estimate of the T_c needs more time to reach its real value.

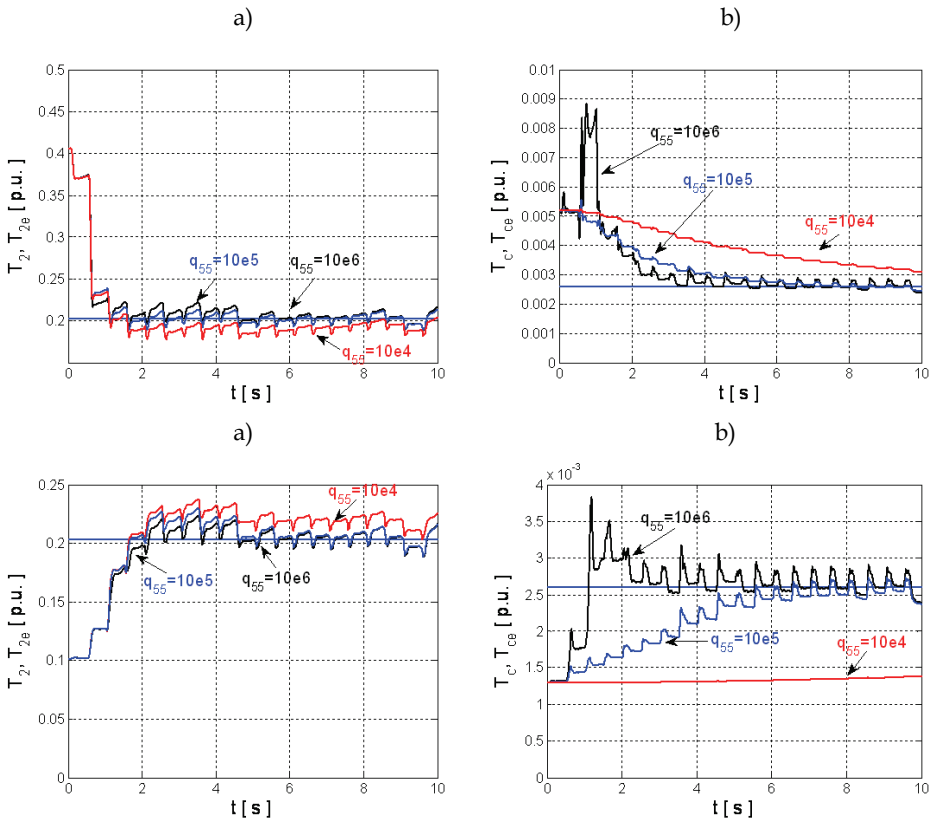


Fig. 11. Transients of the estimated time constant: of load machine (a) and shaft (b) in the case of bigger initial values of those parameters

5.3 Closed-loop control structure (LKF)

The estimated parameters of the two-mass system from the previous section have been used to tune the control structure coefficients according to eq. 5-8. The KF presented in section 3.2 is applied to obtain the information of the shaft torque and the load speed. First the control structure under the reverse condition for the reference speed $\omega_r=0.25$ is tested. The transients of the motor and the load speed for the assumed value of eh damping coefficient $\zeta_r=0.7$ and different value of the resonant frequency are presented in Fig. 12.

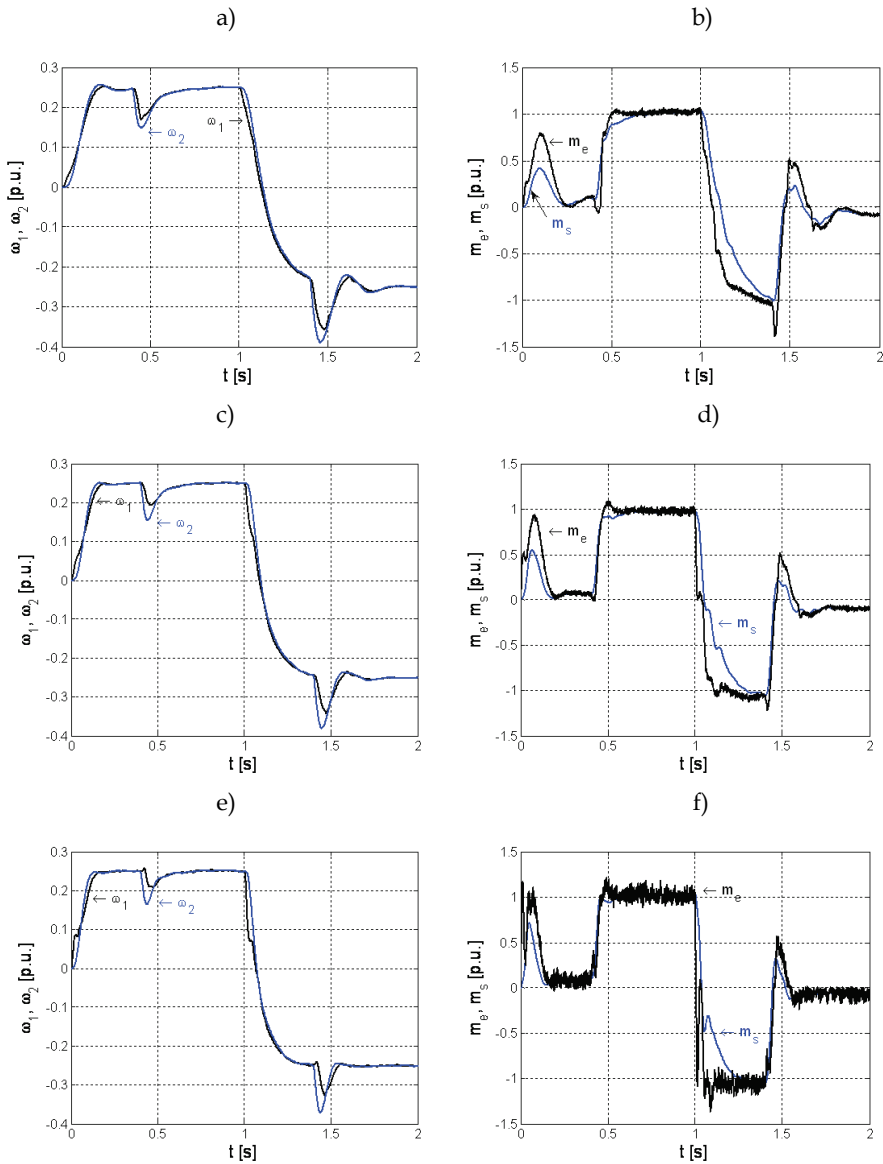


Fig. 12. Experimental transients of the motor and the load speeds (a,c,e) and the electromagnetic and the shaft torques (b,d,f) in the control structure working with the Kalman filter for $\zeta=0.7$ and $\omega_r=30\text{s}^{-1}$ (a,b), $\omega_r=40\text{s}^{-1}$ (c,d) i $\omega_r=50 \text{ s}^{-1}$ (e,f)

The drive system works under the some conditions as described in section 4.2. Similarly as in the simulation study, the faster response of the system is obtained when the value of the resonant frequency is bigger. The level of the noises visible into the electromagnetic torque transients depends also on the assumed dynamic of the control structure. The faster system ,

the bigger amplitude of the noises characterize the system. Next the drive system working for the nominal value of the reference speed $\omega_r=1$ is examined. The transients of the system are shown in Fig. 13.

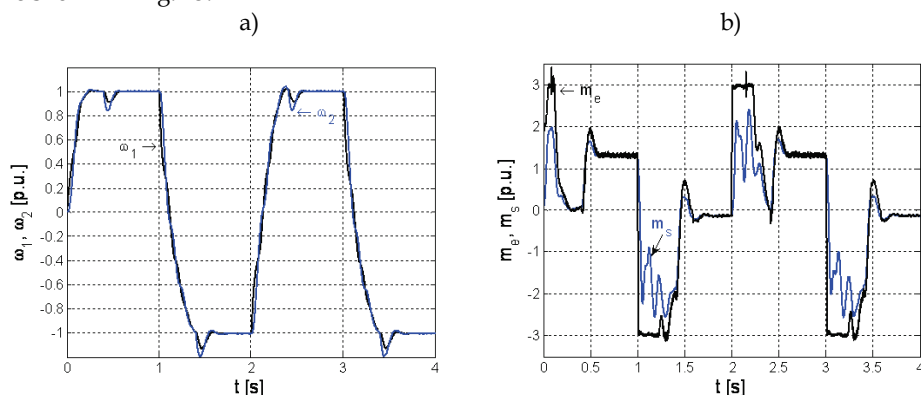


Fig. 13. Experimental transients of the system states for the reference speed $\omega_r=1$

During start-up as well as during the reversal the electromagnetic torque reaches the limitation value (set to 3). The load torque is switched on at the time $t_1=0.4$ and $t_2=2.4$ s and switched off at the time $t_3=1.4$ s and $t_4=2.4$ s. Despite the system is being overloaded the control structure works properly.

6. Conclusion

In the paper the issues related to identification and control of the drive system with an elastic joint has been presented. The NKF is proposed to provide on-line identification of the mechanical parameters of the two-mass system. The time constants of the shaft and the load machine are estimated simultaneously with high accuracy on the basis of the electromagnetic torque and motor speed. These parameters are used to calculate the gain coefficients of the advanced control structure for the two-mass system. Then the control structure with additional feedbacks, which allows to damp the torsional vibrations of the two-mass system effectively, is introduced. In this case the LKF is applied as an estimator of the non-measurable state variables such as the shaft torque, load speed as well as the load torque.

Parameters of the covariance matrices \mathbf{Q} and \mathbf{R} of both considered estimators are selected using the genetic algorithm with special cost functions. The application of the global optimization technique allows to reach the global solution according to the defined cost function. However, the application of the genetic algorithm is possible only as an off-line process due to a long calculation time.

The presented methods are complex and useful of the industrial drive with mechanical elasticity. They allow to ensure the optimal dynamics of the used estimators as well as the whole control structure. The proposed identification and control methods have been examined under simulation and experimental tests. The slight difference between the simulation and experimental results comes from the fact that the additional elements neglected under simulation study such as friction, nonlinear characteristics of the drive exit in the experimental set-up.

7. References

- Angerer B. T., Hintz C. & Schröder D. (2004) Online identification of a nonlinear mechatronic system, *Control Engineering Practice*, Vol. 12, No. , pp. 1465 - 1478.
- Äström K. J. & Hägglund T. (2001) The future of PID control, *Control Engineering Practice*, Vol. 9, No. , pp. 1163-1175.
- Eker I. & Vular M. (2003) Experimental On-Line Identification of a Three-Mass Mechanical System, *Proc. of IEEE Conference on Control Applications CCA 2003*, Istanbul, Turkey, pp. 60-65.
- Erbatur, K., Kaynak, O. & Sabanovic A. (1999). A Study on Robustness Property of Sliding Mode Controllers: A Novel Design and Experimental Investigations, *IEEE Transaction on Industrial Electronics*, Vol. 46, No. 5 , pp. 1012-1018.
- Erenturk, K. (2008). Nonlinear two-mass system control with sliding-mode and optimised proportional and integral derivative controller combined with a grey estimator, *Control Theory & Applications, IET*, Vol. 2, No. 7, pp. 635 - 642.
- Hace, A., Jezernik, K., & Sabanovic, A. (2006). SMC With Disturbance Observer for a Linear Belt Drive, *IEEE Transaction on Industrial Electronics*, Vol. 53, No. 6, pp. 3402-3412.
- Hamamoto, K., Fukuda, T. & Sugie, T. (2003). Iterative feedback tuning of controllers for a two-mass-spring system with friction, *Control Engineering Practice*, Vol. 11, No. 9, pp. 1061-1068.
- Hirovonen, M., Pyrhonen, O. & Handroos H. (2006). Adaptive nonlinear velocity controller for a flexible mechanism of a linear motor, *Mechatronic, Elsevier*, Vol. 16, No. 5, pp. 279-290.
- Hori, Y., Sawada, H., & Chun, Y. (1999). Slow resonance ratio control for vibration suppression and disturbance rejection in torsional system, *IEEE Transaction on Industrial Electronics*, Vol. 46, No. 1, pp. 162-168.
- Katsura, S. & Ohnishi, K. (2005). Force Servoing by Flexible Manipulator Based on Resonance Ratio Control, *Proc. of the IEEE International Symposium on Industrial Electronics ISIE 2005*, Croatia, pp. 1343-1348.
- Nordin, M. & Gutman, P. O. (2002), Controlling Mechanical Systems with Backlash - a Survey, *Automatica*, Vol. 38, No. 10, pp. 1633-1649.
- Orlowska-Kowalska, T. & Szabat, K. (2008). Damping of Torsional Vibrations in Two-Mass System Using Adaptive Sliding Neuro-Fuzzy Approach, *IEEE Transactions on Industrial Informatics*, Vol. 4, No. 1, pp. 47-57.
- O'Sullivan, T., Bingham, C. C. & Schofield, N. (2007). Enhanced Servo-Control Performance of Dual-Mass System, *IEEE Transaction on Industrial Electronics*, Vol. 54, No. 3, pp. 1387-1398.
- Pittner, J., & Simaan, M. A. (2008). Control of a continuous tandem cold metal rolling process, *Control Engineering Practice*, Vol. 16, No. 11, pp. 1379- 1390.
- Schröder D., Hintz C. & Rau M. (2001) Intelligent Modeling, Observation, and Control for Nonlinear Systems, *IEEE/ASME Trans. on Mechatronics*, Vol. 6, No. 2, pp. 122-131.
- Schutte F., Beineke S., Grotstollen H., Witkowski U., Ruckert U. & Ruping S. (1997) Structure- and Parameter Identification for a Two-Mass System with Backlash and Friction using Self-Organizing Map, *Proc. of the International Conference of European Power Electronics EPE'97*, Trondheim, Norway, pp. 3.358-3.363.

- Shen, B. H. & Tsai, M. C. (2006). Robust dynamic stiffness design of linear servomotor drives, *Control Engineering Practice*, Vol. 14, No. 11, pp. 1325-1336.
- Szabat, K., & Orłowska-Kowalska, T., (2007). Vibration suppression in two-mass drive system using PI speed controller and additional feedbacks - comparative study, *IEEE Transaction on Industrial Electronics*, Vol. 54, No. 2, pp. 1193-1206.
- Szabat, K. & Orłowska-Kowalska, T. (2008). Performance Improvement of Industrial Drives With Mechanical Elasticity Using Nonlinear Adaptive Kalman Filter, *IEEE Transactions on Industrial Electronics*, Vol. 55, No. 3, pp. 1075-1084.
- Valenzuela, M. A., Bentley, J. M., Villablanca, A., & Lorenz, R. D. (2005). Dynamic compensation of torsional oscillation in paper machine sections, *IEEE Transaction on Industry Applications*, Vol. 41, No. 6, pp. 1458- 1466.
- Vasak, M., Baotic, M., Petrovic, I. & Peric, N. (2007). Hybrid Theory-Based Time-Optimal Control of an Electronic Throttle, *IEEE Transaction on Industrial Electronic*, Vol. 436, No. 3, pp. 1483-1494.
- Wang, L. & Frayman Y. (2002). A dynamically generated fuzzy neural network and its application to torsional vibration control of tandem cold rolling mill spindles, *Engineering Applications of Artificial Intelligence*, Vol. 15, No. 6, pp. 541-550.
- Wertz H., Beineke S., Fröhleke N., Bolognani S., Unterkofler K., Zigliotto M. & Zordan M. (1999) Computer Aided Commissioning of Speed and Position Control for Electrical Drives with Identification of Mechanical Load, *Proc. of the Thirty-Fourth IAS Annual Meeting Industry Applications Conference*, Phoenix, USA, pp. 4.1372-4.2379.
- Zhang, G. & Furusho, J. (2000). Speed Control of Two-Inertia System by PI/PID Control, *IEEE Trans. on Industrial Electronic*, Vol. 47, No. 3, pp. 603-609.



Kalman Filter Recent Advances and Applications

Edited by Victor M. Moreno and Alberto Pigazo

ISBN 978-953-307-000-1

Hard cover, 584 pages

Publisher InTech

Published online 01, April, 2009

Published in print edition April, 2009

The aim of this book is to provide an overview of recent developments in Kalman filter theory and their applications in engineering and scientific fields. The book is divided into 24 chapters and organized in five blocks corresponding to recent advances in Kalman filtering theory, applications in medical and biological sciences, tracking and positioning systems, electrical engineering and, finally, industrial processes and communication networks.

How to reference

In order to correctly reference this scholarly work, feel free to copy and paste the following:

Krzysztof Szabat and Teresa Orłowska-Kowalska (2009). Application of the Kalman Filters in the Self-Commissioning High-Performance Drive System with an Elastic Joint, Kalman Filter Recent Advances and Applications, Victor M. Moreno and Alberto Pigazo (Ed.), ISBN: 978-953-307-000-1, InTech, Available from: http://www.intechopen.com/books/kalman_filter_recent_advances_and_applications/application_of_the_kalman_filters_in_the_self-commissioning_high-performance_drive_system_with_an_el

INTECH

open science | open minds

InTech Europe

University Campus STeP Ri
Slavka Krautzeka 83/A
51000 Rijeka, Croatia
Phone: +385 (51) 770 447
Fax: +385 (51) 686 166
www.intechopen.com

InTech China

Unit 405, Office Block, Hotel Equatorial Shanghai
No.65, Yan An Road (West), Shanghai, 200040, China
中国上海市延安西路65号上海国际贵都大饭店办公楼405单元
Phone: +86-21-62489820
Fax: +86-21-62489821

© 2009 The Author(s). Licensee IntechOpen. This chapter is distributed under the terms of the [Creative Commons Attribution-NonCommercial-ShareAlike-3.0 License](#), which permits use, distribution and reproduction for non-commercial purposes, provided the original is properly cited and derivative works building on this content are distributed under the same license.